

Aluminum-induced changes in the net carbon fixation and carbon decomposition of a nitrogen-fixing cyanobacterium *Trichodesmium erythraeum*

Linbin Zhou (✉ zhoulb@scsio.ac.cn)

South China Sea Institute of Oceanology Chinese Academy of Sciences <https://orcid.org/0000-0001-7230-4116>

Fengjie Liu

University of Liverpool School of Environmental Sciences

Yehui Tan

South China Sea Institute of Oceanology Chinese Academy of Sciences

Claude Fortin

Institut national de la recherche scientifique

Liangmin Huang

South China Sea Institute of Oceanology Chinese Academy of Sciences

Peter G.C. Campbell

Institut national de la recherche scientifique

Research Article

Keywords: iron-aluminum hypothesis, aluminum, *Trichodesmium*, carbon fixation, decomposition, dissolved organic carbon

Posted Date: April 20th, 2023

DOI: <https://doi.org/10.21203/rs.3.rs-2829740/v1>

License: © ⓘ This work is licensed under a Creative Commons Attribution 4.0 International License.

[Read Full License](#)

Abstract

Recent studies suggest aluminum (Al) likely plays a role in the ocean carbon cycle by altering the biological carbon fixation and carbon decomposition of marine diatoms. However, it remains speculative whether Al has similar effects on other ecologically important phytoplankton groups such as the globally important nitrogen-fixing cyanobacterium, *Trichodesmium*. Here we report the influence of Al on carbon fixation and decomposition in non-axenic cultures of *Trichodesmium erythraeum* IMS101 (CCMP 1985). By using radiocarbon, and adding oceanic relevant amounts of dissolved Al (yielding concentrations of 40 and 200 nM) along with non-Al-amended controls, we investigated the changes in particulate organic carbon (POC) of *Trichodesmium* ($> 2 \mu\text{m}$, *Trichodesmium* POC), and free-living bacteria ($0.2\text{--}2 \mu\text{m}$, bacterial POC), and dissolved organic carbon ($< 0.2 \mu\text{m}$, DOC) over a 116-day growth period. The results showed that the rates of increase of POC in the declining growth phase of *T. erythraeum* were significantly higher (by 11–14%) in the Al-enriched treatments than in the control, and this Al-enhanced carbon fixation is consistent with previous observations on marine diatoms. On the other hand, unlike diatoms, the POC from *T. erythraeum* decomposed faster in the Al-enriched treatments during the first decay phase when bacterial POC and DOC increased along with the decomposition of *Trichodesmium* POC. Further addition of the same amounts of Al (again calculated to increase the Al concentration by 40 and 200 nM) was performed on day 71. This treatment was designed to mimic Al supply from sediment after the settling of *Trichodesmium* colonies to the ocean bottom. Following this second addition, the decomposition rate of both *Trichodesmium* POC and DOC slowed down by 20–27% and 31–62%, respectively, during the second decay phase, when DOC and bacterial POC decreased. The study suggests that Al fertilization in the surface ocean via dust deposition may increase the net carbon fixation and nitrogen fixation by *Trichodesmium*, and thus the supply of new nitrogen to the euphotic zone, whereas Al from sediment may decrease the decomposition rate of decaying *Trichodesmium* settled to the ocean bottom.

Introduction

Effects of aluminum (Al) on marine phytoplankton have been attracting increasing attention. Aluminum may enhance carbon fixation in the upper ocean by favoring the growth of certain groups of phytoplankton by facilitating the utilization of dissolved organic phosphorus, iron, and dinitrogen (Liu et al. 2018; Zhou et al. 2018a; Zhou et al. 2016). Also, Al may help preserve biogenic matter from decay and decomposition, which would facilitate the export of the fixed carbon to ocean depths and its sequestration there (Zhou et al. 2018b). These studies have updated the understanding of the roles of Al in marine carbon biogeochemistry. Data from Antarctic ice cores show a link between the high inputs of Al and iron (Fe) through dust deposition and cold glacial climates (Lambert et al. 2008; Martin 1990). On the basis of the above knowledge, the Iron-Aluminum Hypothesis was proposed to highlight the potential importance of Al in the ocean carbon cycle and climate change. As a lesson from nature, ocean Al fertilization has been proposed as a carbon dioxide removal (negative emission) strategy to alleviate global warming (Liu et al. 2018; Zhou et al. 2023; Zhou et al. 2018b).

Further evidence has recently been reported that supports the link between Al input to the ocean and climate change. For example, Al is found to help sequester organic carbon in marine sediment over millions of years (Anderson et al. 2020; Hemingway et al. 2019). Our recent study shows that Al at environmentally relevant low levels (e.g., 40 nM) can not only significantly increase diatom cell size but also decrease the decomposition rate of marine diatom-produced particulate organic carbon (POC) (Zhou et al. 2021). Cell size is an important factor determining POC sinking velocity; cell size and the decomposition rate of POC are dominant factors influencing vertical POC flux and the efficiency of the biological carbon pump (Buesseler et al. 2020; Martin et al. 1987; Miklasz & Denny 2010). An extrapolation from our laboratory data suggests that an increase in the ambient Al concentration to 40 or 200 nM could lead to 1 to 3 orders of magnitude increases in the diatom POC exported to a depth of 1000 m, respectively (Zhou et al. 2021). In this latter paper, we also argued that increases of Al in the range from 20 to 200 nM might have occurred in the Last Glacial Maximum in the upper layer of the Atlantic Ocean, the Mediterranean Sea, and some sites in the Pacific Ocean and the Indian Ocean, as a consequence of the 2- to 3-fold increase in the dust deposition rates during that period (Kienast et al. 2016; Menzel Barraqueta et al. 2020). Twenty-five-fold increases in dust flux in the Southern Ocean in glacial times compared to interglacial times, as estimated by Lambert et al. (2008), likely significantly increased Al concentrations in the Southern Ocean. The enhanced supply of Al may have substantially increased diatom carbon export to ocean depths in most of the world oceans, drawn down CO₂ in the atmosphere, and contributed to the cold climates in glacial times.

However, it remains unclear how Al will influence the decomposition rate of other ecologically important phytoplankton other than marine diatoms. *Trichodesmium* is a globally important planktonic and nitrogen-fixing cyanobacterium that is widespread in the oligotrophic tropical and subtropical oceans (Capone et al. 1997; Zhang et al. 2022). Nitrogen fixation by *Trichodesmium* can contribute substantially to the primary production in oligotrophic oceans (Bergman et al. 2013; Carpenter & Capone 2008; Zehr & Capone 2020). Previous studies showed that Al addition at the level of 200 nM enhanced the growth of *Trichodesmium* and its expression of the nitrogen-fixing gene (*nifH*) in the South China Sea (Liu et al. 2018; Zhou et al. 2018a). However, the beneficial effects of Al addition on the growth of *Trichodesmium* have not been further tested in the lab. It is also still unknown how Al additions will influence the decomposition of *Trichodesmium*-produced organic carbon.

In this study, we used radiocarbon (¹⁴C) labeling to examine the effects of Al addition at environmentally relevant levels on the carbon fixation and carbon decomposition of a model *Trichodesmium* species, *Trichodesmium erythraeum* IMS101 (CCMP 1985), in batch cultures that lasted for 116 days. Dissolved organic carbon (DOC) and POC in the size fractions containing *Trichodesmium* colonies (> 2 μm) and free-living bacteria (0.2–2 μm) were monitored to determine the net carbon fixation and organic carbon decomposition.

Methods And Materials

Cell cultures

Non-axenic cultures of the nitrogen-fixing cyanobacterium *Trichodesmium erythraeum* IMS101 (CCMP 1985) were obtained from the National Center for Marine Algae and Microbiota—Bigelow Laboratory for Ocean Sciences (USA). The cultures were maintained in an artificial seawater Aquil-tricho medium (500–1000 mL) in trace metal clean 1200-mL polycarbonate bottles at 27°C and a light intensity of 100 $\mu\text{mol}/\text{m}^2/\text{s}$ (with a 12 h:12 h light-dark cycle) (Hong et al. 2017).

Preparation Of The Maintenance And Experimental Media

Trace-metal clean artificial seawater (with a residual Al concentration of 24.7 ± 4.0 nM) was used to prepare the Aquil-tricho medium for maintaining *Trichodesmium* cultures and for the experiments. The maintenance medium contained 10 μM phosphate, vitamins (0.37 nM cyanocobalamin, 2.25 nM biotin, and 297 nM thiamine), and trace metals (1.0 μM iron, 20 nM zinc, 18 nM manganese, 8 nM cobalt, 8 nM copper, 100 nM molybdenum, 10 nM selenium, and 20 nM nickel) buffered with 20 μM ethylenediaminetetraacetic acid (EDTA).

To limit the biomass yield and avoid changes in the culture media pH due to CO_2 assimilation by algae, a phosphate concentration of only 200 nM was used in the Aquil-tricho media for the experiments. Trace-metal-grade sodium dihydrogen phosphate monohydrate (99.998%, Puratronic™) was used to prepare the phosphate stock solutions and the media. Experiments were conducted in media enriched with Al (initial concentrations of 40 and 200 nM dissolved Al) and in a control medium with no added Al. The Al concentrations of 40 and 200 nM were set by adding appropriate volumes of 40 and 200 μM AlCl_3 (trace metal grade 99.9995%, Puratonic) stock solutions to the experimental medium, respectively. These stock solutions were prepared in 0.01 M HCl (Optimum grade, Fisher Scientific). The initial pH value (~ 8.1) was the same in all the experimental media. The two Al concentrations of 40 and 200 nM mimic those in the heavily dust-influenced open ocean, and the upper limit of dissolved Al in natural seawater, respectively (Menzel Barraqueta et al. 2020; van Hulst et al. 2013). Radioactive $\text{NaH}^{14}\text{CO}_3$ (3.7×10^8 Bq/mL) was added to the media to attain radioactivity of 180 Bq/mL (7.56×10^7 Bq/mol C) to monitor organic carbon production and fate in the media.

As in our previous study on diatoms in Aquil* medium (Zhou et al. 2021), microwaving was used to sterilize the artificial seawater and the polycarbonate bottles. Syringe filtration (0.2 μm , Millex® GP filter unit) was used to sterilize the stock solutions of phosphate, trace metals, and vitamins. Trace metal clean bottles and tubes were used for preparing the solutions and media. The media were allowed to sit overnight to reach chemical equilibrium before being used in a sterile, particle-free laminar flow hood.

Experimental Designs

Trichodesmium colonies in the maintenance Aquil-tricho medium were transferred to the low-phosphorus Aquil-tricho medium to acclimate for at least 10 generations. *Trichodesmium* in the exponential growth phase (50 mL aliquots) was then transferred to the experimental media enriched with different

concentrations of Al (0, 40, and 200 nM). Three replicates were prepared for each treatment. The experimental cultures in polycarbonate bottles were incubated for 116 days at 27°C with a light intensity of 100 $\mu\text{mol}/\text{m}^2/\text{s}$ (with a 12 h:12 h light-dark cycle), as was used for the maintenance cultures.

Using the filtration methods described in Zhou et al. (2021), we collected ^{14}C -labeled organic carbon in the size fractions of $> 2 \mu\text{m}$ (tricho POC), $0.2\text{--}2 \mu\text{m}$ (bacterial POC), $< 0.2 \mu\text{m}$ (DOC). Specifically, a 20–50 mL sample was collected from each experimental culture after thorough shaking. The POC of *Trichodesmium* colonies and free-living bacteria in the sample were collected by sequential filtration onto polycarbonate membranes with pore sizes of 2 and $0.2 \mu\text{m}$, respectively (Basu & Shaked 2018). *Trichodesmium* colonies on the $2 \mu\text{m}$ membranes and free-living bacteria on the $0.2 \mu\text{m}$ membranes were transferred to the scintillation vials as the samples representative of tricho POC and bacterial POC, respectively. One milliliter of the filtrate from the $0.2 \mu\text{m}$ filtration step was transferred to a scintillation vial as the DOC sample.

One milliliter of diluted hydrochloric acid (HCl, 1%) was added to each POC sample to remove residual inorganic carbon over a 20-min period. Thirty microliters of 4 M HCl solution were added and mixed to remove inorganic carbon in each DOC sample, also over a 20-min period. After the acid treatment, 10 mL of the scintillation cocktail (Ecolume™, MP Biomedicals) was added to each sample and mixed thoroughly by vortexing. The values of POC and DOC were calculated based on the ^{14}C radioactivity measured with a liquid scintillation analyzer (Tri-Carb 2910 TR, Perkin Elmer).

Trichodesmium colonies could have high sinking rates and experience high concentrations of dissolved Al during the decay after settling to the ocean bottom (Ababou et al. 2023; Moran & Moore 1991; Stoffyn-Egli 1982). To mimic the Al supply from ocean sediments after the settling of decayed *Trichodesmium* colonies to the ocean bottom, additional dissolved Al was introduced into the initial treatments that had been amended with 40 or 200 nM Al. These additions, performed on day 71 when DOC and bacterial POC had reached their peaks, raised the Al concentration by 40 or 200 nM (yielding total added concentrations of 80 or 400 nM). The decomposition rates of DOC and POC in different size fractions were compared among treatments during the decay phase. For convenience in the various figures, we have color-coded the results for 0, 40, and 200 nM Al, but in fact for all data points after the re-addition step (71 d) the actual total amended Al concentrations were 0, 80, and 400 nM.

Calculation And Data Analysis

The growth/increase rate of POC was calculated as the slope of the linear regression of natural logarithms of POC with time (d). The decomposition rates of DOC and POC were calculated using the same method.

One-way analysis of variance (ANOVA) was used to compare mean values among treatments. Least-significant-difference pairwise comparisons followed the one-way ANOVA and t-tests were used to compare mean values between the control and Al-enriched treatments. Levene's test was used to test the

homogeneity of variances. If the variance homogeneity hypothesis was violated, non-parametric tests (median test or Jonckheere-Terpstra test) were used to compare mean values among treatments. One-way repeated-measures ANOVA was used to compare mean values of total POC among treatments (Field 2009).

Results

Growth rate and net carbon fixation

The results showed that *Trichodesmium* in Al-enriched treatments had significantly higher mean growth rates than in the control during the declining growth phase (ANOVA, $df = 8$, $p < 0.05$), whereas the growth rate differences among treatments were not significant in the exponential growth phase (ANOVA, $df = 8$, $p > 0.1$) (Fig. 1a, b). The growth phases were divided based on the changes of POC. The exponential growth phase from day 3 to day 11 was characterized by constant high POC growth rates above 0.4 d^{-1} ; while the declining growth phase started from day 11, when the growth rate began to decrease, to day 27 when the growth rate was approaching to zero (Fig. 1a and Fig. S1). POC decreased during the decay phase (Fig. S1).

The higher growth rates led to higher accumulation of total POC in the Al-enriched treatments than the control (Fig. 2). The amount of POC on day 21 increased by 5% and 16% ($p < 0.05$) in the treatments enriched with 40 nM and 200 nM Al, respectively, compared to the control (ANOVA, $df = 8$, $p = 0.053$; median test, $df = 2$, $p = 0.043$) (Fig. 2a). On day 27, the total amount of POC was 10–15% higher in the Al-enriched cultures compared to the control (Fig. 2a). The results of one-way repeated-measures ANOVA showed that there were higher values of total POC in treatments enriched with higher concentrations of Al from day 21 to day 38 (Mauchly's test of sphericity, $p > 0.1$; $F(2, 6) = 3.98$, $p = 0.079$) (Fig. 2a). Tricho POC in the size fraction $> 2 \mu\text{m}$ was also 11–16% higher in the Al-enriched treatments than the control on day 27, although the differences were not statistically significant (ANOVA, $df = 8$, $p > 0.1$) (Fig. 2b). In summary, Al addition to the culture media led to higher net carbon fixation by *Trichodesmium*.

Decomposition of *Trichodesmium* POC and increase of bacterial POC and DOC during the first decay phase

The amount of total POC started to decrease from day 38 (Fig. 2a), whereas tricho POC peaked earlier around day 27 (Fig. 2b). There were two different decay phases (Fig. S1). The first was from day 27 to day 71, during which tricho POC decomposed and bacterial POC and DOC increased (Fig. 2c, d). The second decay phase, from day 71 to day 116, was characterized by the decay of DOC and bacterial POC (Fig. 2c, d). Tricho POC also decomposed further during the second decay phase.

Tricho POC decreased from about 100 to 25 $\mu\text{mol C/L}$ during the first decay phase from day 27 to day 71. Along with the decrease in tricho POC, bacterial POC and its contribution to total POC increased (Fig. 2c; Fig. S2). Bacterial POC increased from about 20 to 46 $\mu\text{mol C/L}$ from day 27 to day 71. As a result, the proportion of bacterial POC to total POC increased from around 15–65% (Fig. S2). In addition, the

increase in bacterial POC led to an increase in total POC from day 27 to day 38, although tricho POC decayed at the same time (Fig. 2a, b).

The DOC remained at low concentrations around 2 $\mu\text{mol C/L}$ during the exponential growth phase (on day 11) and the early declining growth phase (on day 15) (Fig. S3). However, it increased significantly along with the decay of tricho POC during the first decay phase (Fig. 2d). The DOC concentrations doubled to around 5 $\mu\text{mol C/L}$ on day 21 and day 27, when the concentration of tricho POC peaked (Fig. 2b; Fig. S3). The DOC concentrations increased substantially to around 35 $\mu\text{mol C/L}$ on day 38 and day 54, and to more than 75–150 $\mu\text{mol C/L}$ on day 71 at the end of the first decay phase (Fig. 2d; Fig. S3).

During the first decay phase from day 27 to day 71, the decomposition rates of tricho POC and total POC were significantly higher in the Al-enriched treatments than in the control (ANOVA, $df = 8$, $p < 0.05$) (Fig. 3a, b; Table 1). As a result, the concentrations of tricho POC and total POC left in the cultures were significantly higher in the control than in the Al-enriched treatments on day 71 (ANOVA, $df = 8$, $p < 0.05$). Specifically, the tricho POC and total POC concentrations on day 71 were > 79% and > 28% higher in the control than in the Al-enriched treatments, respectively. DOC concentrations were significantly (18–96%) higher in the control than the Al-enriched treatments on day 71 (median test, $p = 0.043$; Jonckheere-Terpstra, $p = 0.020$). However, the increase rates of bacterial POC during the first decay phase were not significantly different among treatments (ANOVA, $df = 8$, $p > 0.1$) (Fig. 3c). Consistently, the bacterial POC did not significantly differ among the treatments during the entire experiment except for day 71, when the bacterial POC was 6% higher in the control than in the Al-enriched treatments (ANOVA, $df = 8$, $p = 0.051$).

Table 1

Comparisons of the growth, net carbon fixation, and organic carbon decomposition rates (mean \pm standard deviation, $n = 3$) of *Trichodesmium* cultured in Aquil-tricho media enriched or not with Al. The symbols #, *, and ** indicate nearly significant ($0.05 < p < 0.1$), significant ($p < 0.05$), and highly significant ($p < 0.01$) differences compared to the control, respectively. ANOVA, one-way analysis of variance; Nonparametric tests: median and Jonckheere-Terpstra tests.

Parameters	Control	40 nM Al	200 nM Al	ANOVA	Nonparametric tests
Growth rates during the exponential growth phase (days 3–11) (d^{-1})	0.436 \pm 0.004	0.407 \pm 0.024	0.405 \pm 0.028	$p > 0.1$	
Growth rates during the declining growth phase (days 11–27) (d^{-1})	0.141 \pm 0.007	0.157 \pm 0.010*	0.161 \pm 0.004*	$p < 0.05$	
Total POC on day 21 ($\mu\text{mol C/L}$)	94.0 \pm 5.3	99.0 \pm 6.7	108.9 \pm 5.5*	$p = 0.053$	$p < 0.05$
Total POC on day 27 ($\mu\text{mol C/L}$)	117.6 \pm 19.3	129.2 \pm 12.9	134.9 \pm 3.2	$p > 0.1$	
Total POC on day 38 ($\mu\text{mol C/L}$)	134.4 \pm 15.2	136.4 \pm 8.4	145.2 \pm 8.3	$p > 0.1$	
Tricho POC on day 27 ($\mu\text{mol C/L}$)	98.6 \pm 18.4	109.8 \pm 13.1	114.7 \pm 2.0	$p > 0.1$	
Tricho POC on day 38 ($\mu\text{mol C/L}$)	102.5 \pm 17.1	103.5 \pm 7.4	111.4 \pm 10.0	$p > 0.1$	
Total POC decomposition rate (days 38–54) (d^{-1})	0.0005 \pm 0.0020	0.0033 \pm 0.0019	0.0101 \pm 0.0023**	$p = 0.004$	
Total POC decomposition rate (days 54–71) (d^{-1})	0.0267 \pm 0.0047	0.0402 \pm 0.0079*	0.0371 \pm 0.0031*	$p = 0.078$	
Total POC decomposition rate (days 38–71) (d^{-1})	0.0141 \pm 0.0025	0.0225 \pm 0.0047*	0.0242 \pm 0.0022*	$p = 0.021$	
Tricho POC decomposition rate (days 27–54) (d^{-1})	0.0019 \pm 0.0100	0.0074 \pm 0.0025	0.0128 \pm 0.0059**	$p = 0.011$	
Tricho POC decomposition rate (days 54–71) (d^{-1})	0.0559 \pm 0.0082	0.0911 \pm 0.0233*	0.0843 \pm 0.0144#	$p = 0.084$	
Tricho POC decomposition rate (days 27–71) (d^{-1})	0.0218 \pm 0.0038	0.0378 \pm 0.0100*	0.0392 \pm 0.0059*	$p = 0.042$	
Total POC on day 71 ($\mu\text{mol C/L}$)	84.5 \pm 7.1	65.4 \pm 6.2*	65.8 \pm 7.4*	$p = 0.024$	

Parameters	Control	40 nM Al	200 nM Al	ANOVA	Nonparametric tests
Tricho POC on day 71 ($\mu\text{mol C/L}$)	36.3 \pm 6.1	19.9 \pm 6.8*	20.2 \pm 6.2*	p = 0.031	
Bacterial POC on day 71 ($\mu\text{mol C/L}$)	48.2 \pm 1.0	45.5 \pm 0.7*	45.6 \pm 1.6*	p = 0.051	
DOC on day 71 ($\mu\text{mol C/L}$)	149.4 \pm 19.3	127.0 \pm 45.9	76.3 \pm 11.7*	p = 0.056	p < 0.05
Bacterial POC increase rate (days 27–71) (d^{-1})	0.0196 \pm 0.0016	0.0178 \pm 0.0014	0.0171 \pm 0.0025	p > 1.0	
Total POC decomposition rate (days 71–116) (d^{-1})	0.0155 \pm 0.0007	0.0124 \pm 0.0020*	0.0107 \pm 0.0008**	p = 0.010	
Tricho POC decomposition rate (days 71–116) (d^{-1})	0.0353 \pm 0.0005	0.0284 \pm 0.0085	0.0258 \pm 0.0011**	p > 0.1	p < 0.05
Bacterial POC decomposition rate (days 71–116) (d^{-1})	0.0072 \pm 0.0003	0.0078 \pm 0.0007	0.0063 \pm 0.0006	p = 0.050	p > 0.1
DOC decomposition rate (days 71–116) (d^{-1})	0.0267 \pm 0.0039	0.0183 \pm 0.0054#	0.0102 \pm 0.0060**	p = 0.022	

Decomposition of DOC and POC during the second decay phase with mimicked re-supply of dissolved Al from sediment resuspension

The concentrations of DOC and bacterial POC started to decrease during the second decay phase after day 71, and total POC and tricho POC decomposed further (Fig. 2). The proportion of bacterial POC to total POC increased to more than 80% (Fig. S2).

Significantly lower decomposition rates of DOC and POC were observed in Al-enriched treatments than in the control during the second decay phase after the re-addition of Al on day 71 (Fig. 4). The DOC decomposition rates were 31–62% lower in the Al-enriched media than in the control (ANOVA, df = 8, p < 0.02). Tricho POC decomposition rates in the Al-enriched treatments declined rapidly by more than 50% after the re-addition of Al, whereas those in the control remained at relatively high values (Fig. S4). As a result, tricho POC decomposition rates during the second decay phase were 20–26% lower in the Al-enriched treatments than in the control (median test and Jonckheere-Terpstra test, p < 0.05). However, the bacterial POC decomposition rates did not significantly differ between the control and Al-enriched treatments (median test and Jonckheere-Terpstra test, p > 0.1). There were also no significant differences in bacterial POC among treatments after day 71 (median test or Jonckheere-Terpstra test, p > 0.1)

(Fig. 2c). As a result, total POC decomposition rates were 20–31% lower in the Al-enriched treatments than in the control (ANOVA, $df = 8$, $p = 0.01$). These results suggest that the mimicked re-supply of dissolved Al from sediment resuspension may significantly decrease the decomposition rates of organic carbon related to decaying *Trichodesmium* colonies settled to the ocean bottom.

Discussion

Amendments resulting in Al concentrations of 40 and 200 nM significantly increased the growth rates of *Trichodesmium* during the declining growth phase and net carbon fixation by the cyanobacterium in the Aquil-tricho medium. However, the *Trichodesmium*-produced POC decomposed and was remineralized more rapidly in the Al-enriched treatments than in the control during the first decay phase from day 27 to day 71, when increases in bacterial POC and DOC accompanied the decomposition of tricho POC. After the re-addition of Al at day 71, to mimic Al supply from sediment resuspension after the settling of decaying *Trichodesmium* colonies to the ocean bottom, the decomposition rates of DOC, tricho POC, and total POC slowed significantly during the second decay phase, when DOC and bacterial POC decreased.

This study provides new data to help understand the roles of Al in the ocean carbon cycle, focusing on the globally important nitrogen-fixing cyanobacterium *Trichodesmium*. These data also add new support for the iron-aluminum hypothesis, which suggests that Al inputs to the ocean increase marine carbon sinks and influence climate change by impacting carbon fixation in the upper ocean, carbon export to the ocean interior, and carbon sequestration in the deep ocean depths and sediments (Zhou et al. 2023; Zhou et al. 2021; Zhou et al. 2018b)

Beneficial effects of Al on the growth and carbon fixation by marine phytoplankton

The beneficial effects of Al addition on the growth and net carbon fixation of *Trichodesmium* in the present study are consistent with previous results showing Al effects on marine nitrogen-fixing cyanobacteria. Previous field studies showed that Al addition enhanced the growth of *Trichodesmium*, the expression of its nitrogen-fixing gene (*nifH*), and the nitrogen fixation rate in the South China Sea (Liu et al. 2018; Zhou et al. 2018a). A laboratory study reported the beneficial effects of Al addition on the growth and nitrogen fixation of a unicellular nitrogen-fixing cyanobacterium *Crocospaera watsonii* under phosphorus-deficient conditions (Liu et al. 2018), although high concentrations of Al could be toxic to the same species under phosphorus-sufficient conditions (Liu et al. 2020). The present study adds laboratory experimental support for the evidence of the beneficial effects of Al on *Trichodesmium* in field studies.

The beneficial effects of Al in the present study are also consistent with previous studies on other marine phytoplankton (Zhou et al. 2021). The beneficial effects of Al on the growth of marine phytoplankton (including diatoms, chlorophytes, and non-nitrogen-fixing cyanobacteria) have been summarized in previous studies (Zhou et al. 2021; Zhou et al. 2018b). These show that the beneficial effects of Al on marine phytoplankton were sporadically reported during the 1960s to the 2000s, and increasingly reported in the more recent literature. The beneficial effects of Al on marine diatoms and cyanobacteria and the underlying mechanisms have been closely examined in recent years (Liu et al. 2018; Zhou et al.

2016). Both the present study and previous studies on marine diatoms showed that the beneficial effects occurred in the declining growth phase when phosphorus limitation occurred (Zhou et al. 2021). Our recent study shows that the presence of Al at the same concentrations (40 and 200 nM) used in the present study increased the net carbon fixation of three marine diatoms by 9–29% in Aquil* medium with only 100 nM phosphate (Zhou et al. 2021). In the present work, we observed that similar Al additions increased net carbon fixation of *Trichodesmium* by 11–16% in Aquil-tricho media with 200 nM phosphate (Fig. 1c, d)

The mechanisms underlying the beneficial effects of Al on *Trichodesmium's* carbon fixation are open to discussion. A recent study has identified novel metallophores with a high affinity for Al in *Trichodesmium erythraeum* colonies from the Gulf of Aqaba, and these metallophores were suggested to be linked to the use of dust as a source of nutrients (Gledhill et al. 2019). However, whether the concentration of dissolved Al can affect the metallophores, and if they are related to the observed beneficial effects of Al, remains unknown. Enhanced use of dissolved organic phosphorus, involving an increased efficiency of alkaline phosphatase, has been proposed as a mechanism underlying the beneficial effects (Zhou et al. 2021; Zhou et al. 2016). Given the low initial phosphate concentration (200 nM) and sufficient concentrations of dinitrogen and nutrients including trace metals in the Aquil-tricho medium, phosphorus should be the only nutrient that limited the growth of the nitrogen-fixing cyanobacterium in the declining growth phase. We hypothesize that a similar mechanism for enhancing phosphorus use may support the increased growth of *Trichodesmium* in the present study. Further work is needed to evaluate this hypothesis.

Influences of Al on organic carbon decomposition

The higher decomposition rates of tricho POC in the Al-enriched treatments compared to the control differ from the results of previous studies on marine diatoms. Earlier studies have shown that the incorporation of Al into the frustules of marine diatoms can decrease their solubility and hinder the release of the associated organic carbon (Abramson et al. 2009; Dixit et al. 2001; Van Cappellen et al. 2002). Our recent study demonstrates that Al additions to achieve environmentally relevant low levels of 40 and 200 nM significantly slowed down the decomposition rates of the diatom-produced POC, by up to 58% (Zhou et al. 2021). In contrast, the decomposition rates of tricho POC were > 70% higher in the Al-enriched treatments compared to the control in the present study (Fig. 3; Table 1). This difference indicates that the Al impacts on phytoplankton-POC decomposition may vary among different taxa. Further work is needed to examine the Al impacts on other major phytoplankton classes such as dinoflagellates and coccolithophores.

The lower DOC accumulation in the Al-enriched treatments compared to the control during the first decay phase suggests that tricho POC decomposed and was remineralized more quickly in the presence of Al (Fig. 2d; Table 1). DOC and bacterial POC accumulated along with the decomposition of tricho POC during the first decay phase (Fig. 2). This suggests that part of the decomposed tricho POC was transformed into DOC and bacterial POC. The other part of the decomposed POC was presumably remineralized to inorganic carbon. Generally, as more POC decomposed, more DOC and bacteria POC

accumulated. However, lower accumulation of DOC was observed in the Al-enriched treatments compared to the control at the end of the first decay phase on day 71 (Fig. 2d; Table 1). This lower accumulation was observed despite the more rapid decomposition of tricho POC in the Al-enriched treatments than the control during the first decay phase (Fig. 3a). These results suggest that during the first decay phase, the proportion of tricho POC that was transformed into inorganic carbon was higher in the Al-enriched treatments than in the controls. The underlying mechanisms for the quick decomposition and remineralization of tricho POC in the Al-enriched treatments are unknown. Since we did not observe higher bacterial biomass (POC) in the Al-enriched treatments compared to the control (Fig. 2c), this may rule out differences in bacteria activity as the reason for the fast decomposition of tricho POC in the Al-enriched treatments. The present results suggest that Al may influence tricho POC decomposition with very different mechanisms, compared to the Al influence on diatom POC decomposition. Additional research is needed to explore the underlying mechanisms involved.

The present study showed that the decomposition rates of DOC slowed during the second decay phase (Fig. 4), i.e., after the re-addition of Al to mimic Al supply after the settling of decaying *Trichodesmium* colonies to the ocean depth. (Fig. 4). There were also no significant differences in the bacteria biomass among treatments during the second decay phase. These results suggest that DOC released by Al-treated *Trichodesmium* was more difficult to decompose, or that Al treatment may make DOC released by *Trichodesmium* more difficult to decompose. Future studies are needed to assess these hypotheses.

Interestingly, our results indicate that the re-addition of Al in the *Trichodesmium* decay phase may also affect the rate of POC decomposition (Fig. 4). Significantly lower POC decomposition rates were observed in the Al-enriched treatment than in the control during the second decay phase (Fig. 4). One interpretation of this observation is that the added Al reacted with the decayed *Trichodesmium* and slowed down the tricho POC decomposition rates. Rapid decreases in the tricho POC decomposition rates were indeed observed in the Al-enriched treatments after the re-addition of Al (Fig. S4). A second possible explanation would be that the tricho POC left after the first decay phase was more refractory in the Al-enriched treatments than in the control. We indeed found that tricho POC remaining on day 71 was significantly less in the Al-enriched treatments than in the control (Table 1; Fig. 2). The residual tricho POC remaining in the Al-enriched treatments could be more refractory than that in the control treatment. Detailed examination of tricho POC decomposition rates showed that there was also a quick drop in decomposition rates in the control during the period from days 96–116, when only refractory POC remained (Fig. S4). The presence of refractory POC and the effects of Al re-addition together may have led to the significant slowing down of the tricho POC decomposition rates in the Al-enriched treatments after day 71.

Since the re-addition of Al to some extent mimicked high Al concentrations experienced by decaying *Trichodesmium* settled to the ocean interior, we speculate that the high concentrations of dissolved Al in seawater near the ocean bottom, and in interstitial waters in sediments (Moran & Moore 1991; Stoffyn-Egli 1982) may play roles in preserving organic carbon related to *Trichodesmium* colonies settled to the ocean bottom. The roles of Al, as well as Fe in carbon storage, are becoming increasingly understood in

soils (Merino et al. 2017; Wagai et al. 2020). However, their roles in marine sediments are still unclear. To understand the roles of Al in preserving organic carbon in marine sediments, further research is needed to simulate the low temperature, darkness, and microbial environments in the ocean interior or sediment.

Implications for the ocean carbon and nitrogen cycles and the biological carbon pump

Our results suggest that Al inputs may enhance net nitrogen fixation and carbon fixation in the oligotrophic subtropical and tropical upper oceans, where nitrogen is often limited and nitrogen-fixing cyanobacteria such as *Trichodesmium* are prevalent and contribute to the biological carbon pump.

First, Al addition could directly increase the net carbon fixation of *Trichodesmium*, which is an important class of phytoplankton in the oligotrophic subtropical and tropical upper oceans. Second, higher net carbon fixation by *Trichodesmium* would also mean higher new nitrogen input to all the phytoplankton in the upper ocean, because *Trichodesmium* can use dinitrogen and transform it into reactive new nitrogen. A high proportion of the fixed reactive nitrogen would be released and used by other non-nitrogen-fixing phytoplankton such as diatoms (Bronk & Steinberg 2008). Our results indicate that Al concentrations at the levels of 40 and 200 nM not only increased net nitrogen fixation but might also benefit the transfer of the fixed reactive nitrogen to other phytoplankton, given that *Trichodesmium* decomposed and remineralized more rapidly in the Al-enriched treatments than in the control media. The remineralized nitrogen may support carbon fixation by other phytoplankton species such as diatoms and thus increase overall carbon fixation in the upper ocean.

By using the experimental data obtained in the present study, we can roughly estimate the effects of natural Al fertilization from dust deposition and sediment resuspension (Fig. 5). Dust deposition into *Trichodesmium*-inhabited seawaters, such as the northern Atlantic Ocean and the Red Sea (Benaltabet et al. 2022; Menzel Barraqueta et al. 2020), can result in high concentrations of dissolved Al, comparable to those used in the present study. We estimate that Al fertilization through dust deposition could increase the total *Trichodesmium*-released nitrogen in the euphotic zone by 11–19%, and increase by 11–17% the carbon fixation of *Trichodesmium* and other phytoplankton supported by the *Trichodesmium*-released nitrogen, and increase by 6–13% the *Trichodesmium* POC exported to below 100 m in depth (Fig. 5). The estimates were based on the present experimental data and reported knowledge in the literature: 1) the Al fertilization at the levels of 40 and 200 nM from dust deposition is assumed to increase the net carbon fixation (nitrogen fixation) in *Trichodesmium* biomass by 10–15% (Fig. 1 and Table 1), and *Trichodesmium* is assumed to release 50% of its fixed nitrogen during its growth in the euphotic zone (Bronk & Steinberg 2008), i.e., the released nitrogen during growth is equal to the net nitrogen fixation in *Trichodesmium* biomass; 2) the *Trichodesmium* colonies will release additional reactive nitrogen to the euphotic zone before they sink out of the euphotic zone, and all the nitrogen released in the euphotic zone will be used by marine phytoplankton for carbon fixation with a Redfield reference C:N ratio (6.6) similar to that of *Trichodesmium* (White et al. 2006); 3) the sinking *Trichodesmium* colonies will deposit to the deep ocean with sinking rates between 50–100 m/d (Ababou et al. 2023; Coles et al. 2004), and the Al treated *Trichodesmium* will decompose during the sinking with higher rates (by 73–80%) as observed in

the present study. The rough estimates suggest that Al fertilization could benefit nitrogen fixation by *Trichodesmium*, nitrogen supply to the euphotic zone, and thus enhance total carbon fixation in the upper ocean and carbon export to ocean interiors.

After being exported to the ocean interior, the re-supply of dissolved Al from sediment resuspension could decrease the decomposition rates of POC (by 20–27%) and DOC (by 31–62%) related to the decaying *Trichodesmium* colonies. In other words, the Al from sediment may help to preserve organic carbon in the settled *Trichodesmium*.

In summary, our study suggests that Al fertilization from dust deposition to the oligotrophic subtropical and tropical upper oceans could increase the net carbon fixation of *Trichodesmium*, the *Trichodesmium*-mediated nitrogen supply to the euphotic zone, and carbon export to below 100 m in depth. In addition, Al supply from sediment resuspension may help to preserve the organic carbon of *Trichodesmium* colonies settled in ocean interiors and sediments. Therefore, this study provides additional support for the iron-aluminum hypothesis.

Declarations

Acknowledgments and Funding

We thank Kim Racine and Lise Rancourt at the Institut national de la Recherche scientifique for their technical assistance. We also thank the data archive support from the National Earth System Data Center, National Science & Technology Infrastructure of China ([http:// www.geodata.cn](http://www.geodata.cn)). This work was supported by the National Natural Science Foundation of China (41506150), the Natural Sciences and Engineering Research Council of Canada (NSERC), the Guangdong Basic and Applied Basic Research Foundation (2019A1515011645), the Development Fund of South China Sea Institute of Oceanology of the Chinese Academy of Sciences (SCSIO202204), the Science and Technology Planning Project of Guangdong Province, China (2020B1212060058). C. Fortin and P. G. C. Campbell were supported by the Canada Research Chairs Program. L. Zhou was supported by a Chinese Academy of Sciences Scholarship. F. Liu is supported by the European Union's Horizon 2020 research and innovation programme under the Marie Skłodowska-Curie grant agreement No 891418 and UK Natural Environment Research Council Grant NE/V01451X/1.

Competing Interests

The authors have no conflicts of interest to disclose.

Author Contributions

All authors contributed to the study conception and design. Material preparation, data collection, and analysis were performed by Linbin Zhou and Fengjie Liu. The first draft of the manuscript was written by Linbin Zhou and all authors commented on previous versions of the manuscript. All authors read and approved the final manuscript.

Data Availability

Data for this manuscript are available at the South China Sea Ocean Data Center, National Earth System Science Data Center, National Science & Technology Infrastructure of China (<http://data.scsio.ac.cn/metaData-detail/1646764363844362240>).

References

1. Ababou F-E, Le Moigne FAC, Grosso O, Guigue C, Nunige S, Camps M, Bonnet S (2023) Mechanistic understanding of diazotroph aggregation and sinking: “A rolling tank approach”. *Limnology and Oceanography* 68(3): 666-677
2. Abramson L, Wirick S, Lee C, Jacobsen C, Brandes JA (2009) The use of soft X-ray spectromicroscopy to investigate the distribution and composition of organic matter in a diatom frustule and a biomimetic analog. *Deep-Sea Research II* 56(18): 1369-1380
3. Anderson RP, Tosca NJ, Cinque G, Frogley MD, Lekkas I, Akey A, Hughes GM, Bergmann KD, Knoll AH, Briggs DEG (2020) Aluminosilicate haloes preserve complex life approximately 800 million years ago. *Interface Focus* 10(4): 20200011
4. Basu S, Shaked Y (2018) Mineral iron utilization by natural and cultured *Trichodesmium* and associated bacteria. *Limnology and Oceanography* 63(6): 2307-2320
5. Benalabet T, Lapid G, Torfstein A (2022) Dissolved aluminium dynamics in response to dust storms, wet deposition, and sediment resuspension in the Gulf of Aqaba, northern Red Sea. *Geochimica et Cosmochimica Acta* 335: 137-154
6. Bergman B, Sandh G, Lin S, Larsson J, Carpenter EJ (2013) *Trichodesmium*– a widespread marine cyanobacterium with unusual nitrogen fixation properties. *FEMS Microbiology Reviews* 37(3): 286-302
7. Bronk DA, Steinberg DK (2008) Chapter 8 - Nitrogen Regeneration. In: Capone DG, Bronk DA, Mulholland MR & Carpenter EJ (eds) *Nitrogen in the Marine Environment (Second Edition)*. Academic Press, San Diego. p 385-467
8. Buesseler KO, Boyd PW, Black EE, Siegel DA (2020) Metrics that matter for assessing the ocean biological carbon pump. *Proceedings of the National Academy of Sciences* 117(18): 9679-9687
9. Capone DG, Zehr JP, Paerl HW, Bergman B, Carpenter EJ (1997) *Trichodesmium*, a globally significant marine cyanobacterium. *Science* 276: 1221-1229
10. Carpenter EJ, Capone DG (2008) Chapter 4 - Nitrogen Fixation in the Marine Environment. In: Capone DG, Bronk DA, Mulholland MR & Carpenter EJ (eds) *Nitrogen in the Marine Environment (Second Edition)*. Academic Press, San Diego. p 141-198
11. Coles VJ, Hood RR, Pascual M, Capone DG (2004) Modeling the impact of *Trichodesmium* and nitrogen fixation in the Atlantic Ocean. *Journal of Geophysical Research: Oceans* 109(C6): C06007
12. Dixit S, Van Cappellen P, van Bennekom AJ (2001) Processes controlling solubility of biogenic silica and pore water build-up of silicic acid in marine sediments. *Marine Chemistry* 73(3–4): 333-352

13. Field AP (2009) *Discovering Statistics Using SPSS (and sex and drugs and rock 'n' roll)*. SAGE Publications Ltd, Singapore
14. Gledhill M, Basu S, Shaked Y (2019) Metallophores associated with *Trichodesmium erythraeum* colonies from the Gulf of Aqaba. *Metallomics* 11(9): 1547-1557
15. Hemingway JD, Rothman DH, Grant KE, Rosengard SZ, Eglinton TI, Derry LA, Galy VV (2019) Mineral protection regulates long-term global preservation of natural organic carbon. *Nature* 570(7760): 228-231
16. Hong H, Shen R, Zhang F, Wen Z, Chang S, Lin W, Kranz SA, Luo Y-W, Kao S-J, Morel FMM, Shi D (2017) The complex effects of ocean acidification on the prominent N₂-fixing cyanobacterium *Trichodesmium*. *Science* 356(6337): 527-531
17. Kienast SS, Winckler G, Lippold J, Albani S, Mahowald NM (2016) Tracing dust input to the global ocean using thorium isotopes in marine sediments: ThoroMap. *Global Biogeochemical Cycles* 30(10): 1526-1541
18. Lambert F, Delmonte B, Petit JR, Bigler M, Kaufmann PR, Hutterli MA, Stocker TF, Ruth U, Steffensen JP, Maggi V (2008) Dust-climate couplings over the past 800,000 years from the EPICA Dome C ice core. *Nature* 452(7187): 616-619
19. Liu J, Zhou L, Ke Z, Li G, Tan Y (2020) Phosphorus deficiency induced by aluminum in a marine nitrogen-fixing cyanobacterium *Crocospaera watsonii* WH0003. *Chemosphere* 246: 125641
20. Liu J, Zhou L, Li G, Ke Z, Shi R, Tan Y (2018) Beneficial effects of aluminum enrichment on nitrogen-fixing cyanobacteria in the South China Sea. *Marine Pollution Bulletin* 129(1): 142–150
21. Martin JH (1990) Glacial-interglacial CO₂ change: The Iron Hypothesis. *Paleoceanography* 5(1): 1-13
22. Martin JH, Knauer GA, Karl DM, Broenkow WW (1987) VERTEX: carbon cycling in the northeast Pacific. *Deep Sea Research Part A. Oceanographic Research Papers* 34(2): 267-285
23. Menzel Barraqueta J-L, Samanta S, Achterberg EP, Bowie AR, Croot P, Cloete R, De Jongh T, Gelado-Caballero MD, Klar JK, Middag R, Looock JC, Remenyi TA, Wenzel B, Roychoudhury AN (2020) A first global oceanic compilation of observational dissolved aluminum data with regional statistical data treatment. *Frontiers in Marine Science* 7: 468
24. Merino C, Fontaine S, Palma G, Matus F (2017) Effect of aluminium on mineralization of water extractable organic matter and microbial respiration in southern temperate rainforest soils. *European Journal of Soil Biology* 82: 56-65
25. Miklasz KA, Denny MW (2010) Diatom sinking speeds: Improved predictions and insight from a modified Stokes' law. *Limnology and Oceanography* 55(6): 2513-2525
26. Moran SB, Moore RM (1991) The potential source of dissolved aluminum from resuspended sediments to the North Atlantic Deep Water. *Geochimica et Cosmochimica Acta* 55(10): 2745-2751
27. Stoffyn-Egli P (1982) Dissolved aluminium in interstitial waters of recent terrigenous marine sediments from the North Atlantic Ocean. *Geochimica et Cosmochimica Acta* 46(8): 1345-1352

28. Van Cappellen P, Dixit S, van Beusekom J (2002) Biogenic silica dissolution in the oceans: Reconciling experimental and field-based dissolution rates. *Global Biogeochemical Cycles* 16(4): 1075
29. van Hulst M, Sterl A, Tagliabue A, Dutay JC, Gehlen M, de Baar HJW, Middag R (2013) Aluminium in an ocean general circulation model compared with the West Atlantic Geotraces cruises. *Journal of Marine Systems* 126: 3-23
30. Wagai R, Kajiura M, Asano M (2020) Iron and aluminum association with microbially processed organic matter via meso-density aggregate formation across soils: organo-metallic glue hypothesis. *SOIL* 6(2): 597-627
31. White AE, Spitz YH, Karl DM, Letelier RM (2006) Flexible elemental stoichiometry in *Trichodesmium* spp. and its ecological implications. *Limnology and Oceanography* 51(4): 1777-1790
32. Zehr JP, Capone DG (2020) Changing perspectives in marine nitrogen fixation. *Science* 368(6492):
33. Zhang F, Wen Z, Wang S, Tang W, Luo Y-W, Kranz SA, Hong H, Shi D (2022) Phosphate limitation intensifies negative effects of ocean acidification on globally important nitrogen fixing cyanobacterium. *Nature Communications* 13(1): 6730
34. Zhou L, Huang L, Tan Y (2023) Iron-aluminum hypothesis and the potential of ocean aluminum fertilization as a carbon dioxide removal strategy (In Chinese with English abstract). *Journal of Tropical Oceanography*:
35. Zhou L, Liu F, Liu Q, Fortin C, Tan Y, Huang L, Campbell PGC (2021) Aluminum increases net carbon fixation by marine diatoms and decreases their decomposition: Evidence for the iron–aluminum hypothesis. *Limnology and Oceanography* 66(7): 2712-2727
36. Zhou L, Liu J, Xing S, Tan Y, Huang L (2018a) Phytoplankton responses to aluminum enrichment in the South China Sea. *Journal of Inorganic Biochemistry* 181: 117-131
37. Zhou L, Tan Y, Huang L, Fortin C, Campbell PGC (2018b) Aluminum effects on marine phytoplankton: implications for a revised Iron Hypothesis (Iron-Aluminum Hypothesis). *Biogeochemistry* 139(2): 123-137
38. Zhou L, Tan Y, Huang L, Wang W-X (2016) Enhanced utilization of organic phosphorus in a marine diatom *Thalassiosira weissflogii*: A possible mechanism for aluminum effect under P limitation. *Journal of Experimental Marine Biology and Ecology* 478: 77-85

Figures

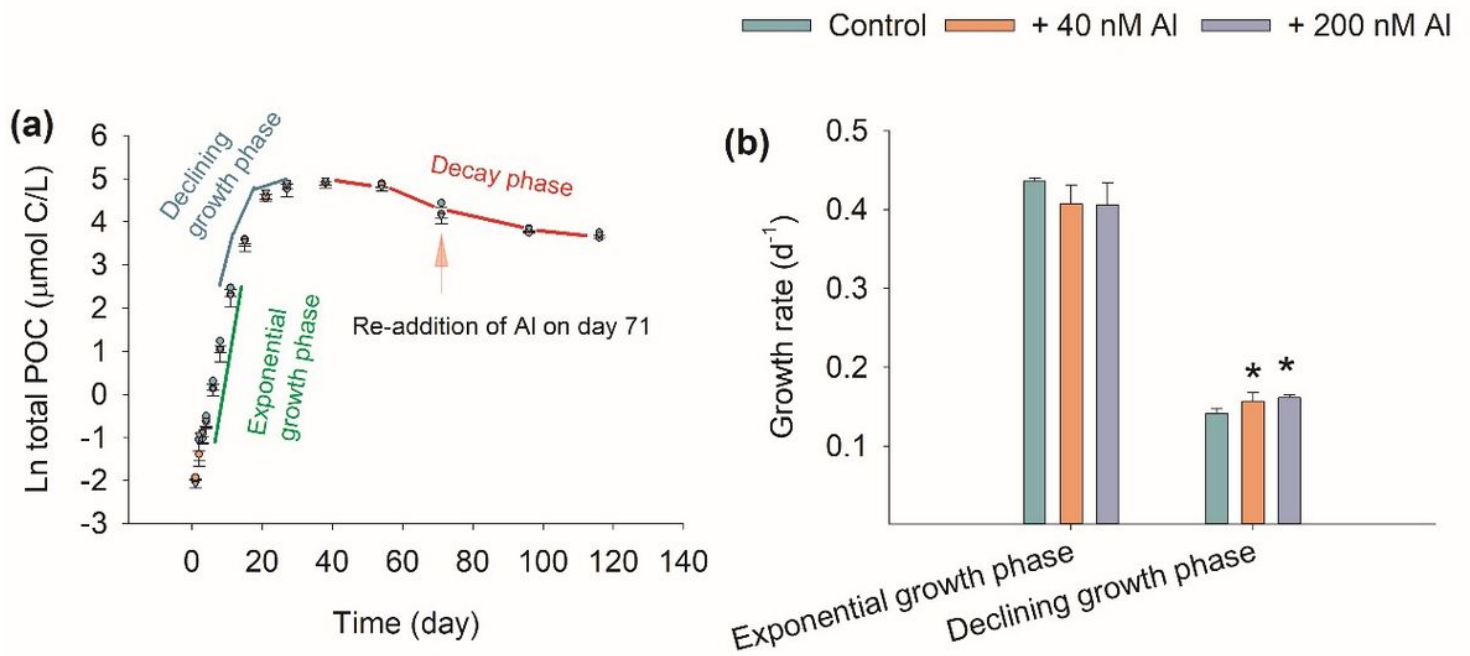


Figure 1

Mean growth rates of total particulate organic carbon (POC) in different growth phases of *Trichodesmium* cultures in Aquil-tricho media enriched with different concentrations of aluminum (Al). (a), the growth phases; (b), growth rates. The error bars represent the standard deviations ($n = 3$). The symbol * indicates the differences between the Al-enriched treatment and the control were significant ($p < 0.05$).

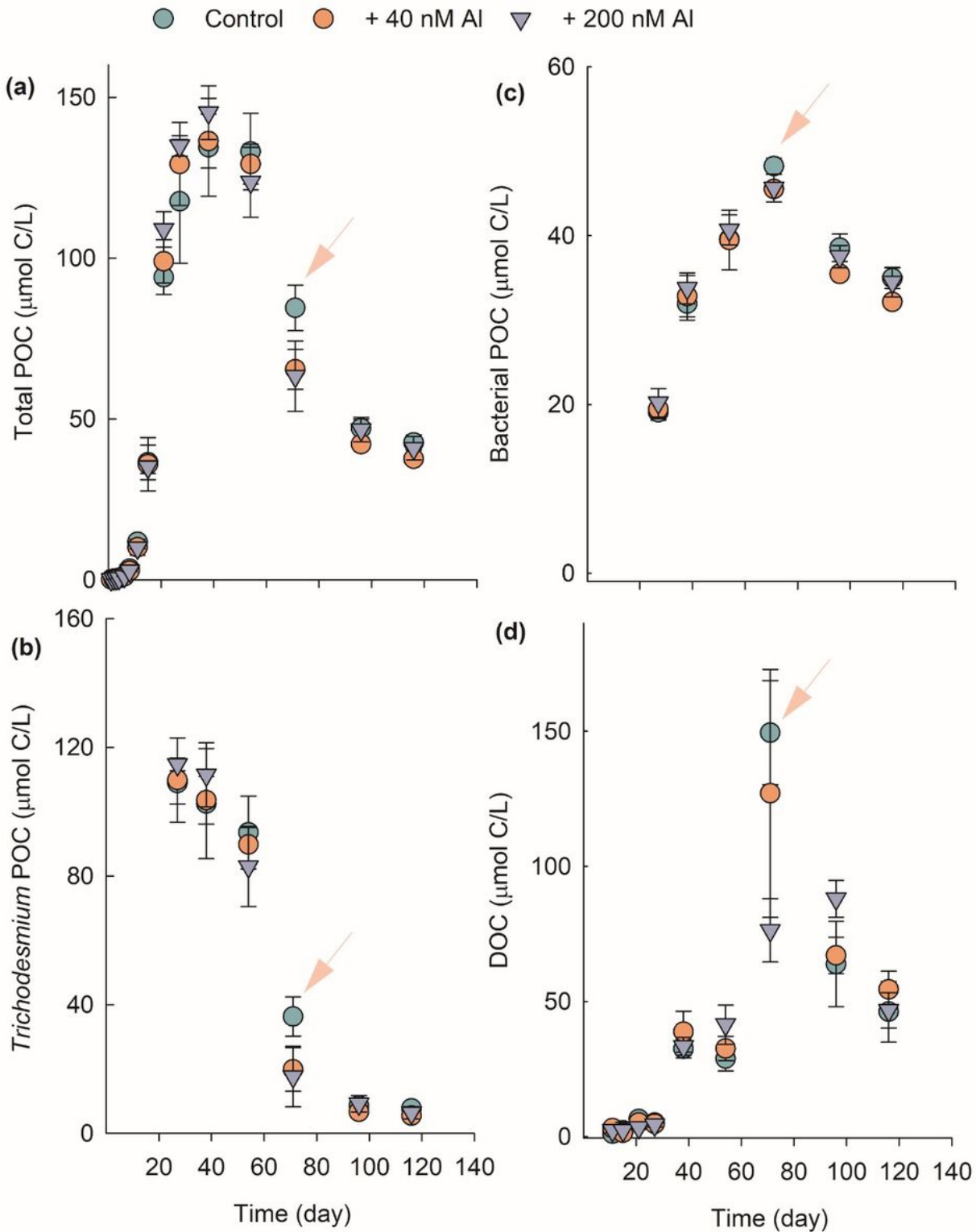


Figure 2

Changes of organic carbon in *Trichodesmium* cultures in Aquil-tricho media enriched with different concentrations of aluminum (Al). (a), total particulate organic carbon (POC); (b), *Trichodesmium* POC in the fraction > 2 μm ; (c) bacterial POC in the fraction of 0.2–2 μm ; and (d), dissolved organic carbon (DOC). The error bars represent the standard deviations (n = 3). The arrows indicate the re-addition of Al on day 71.

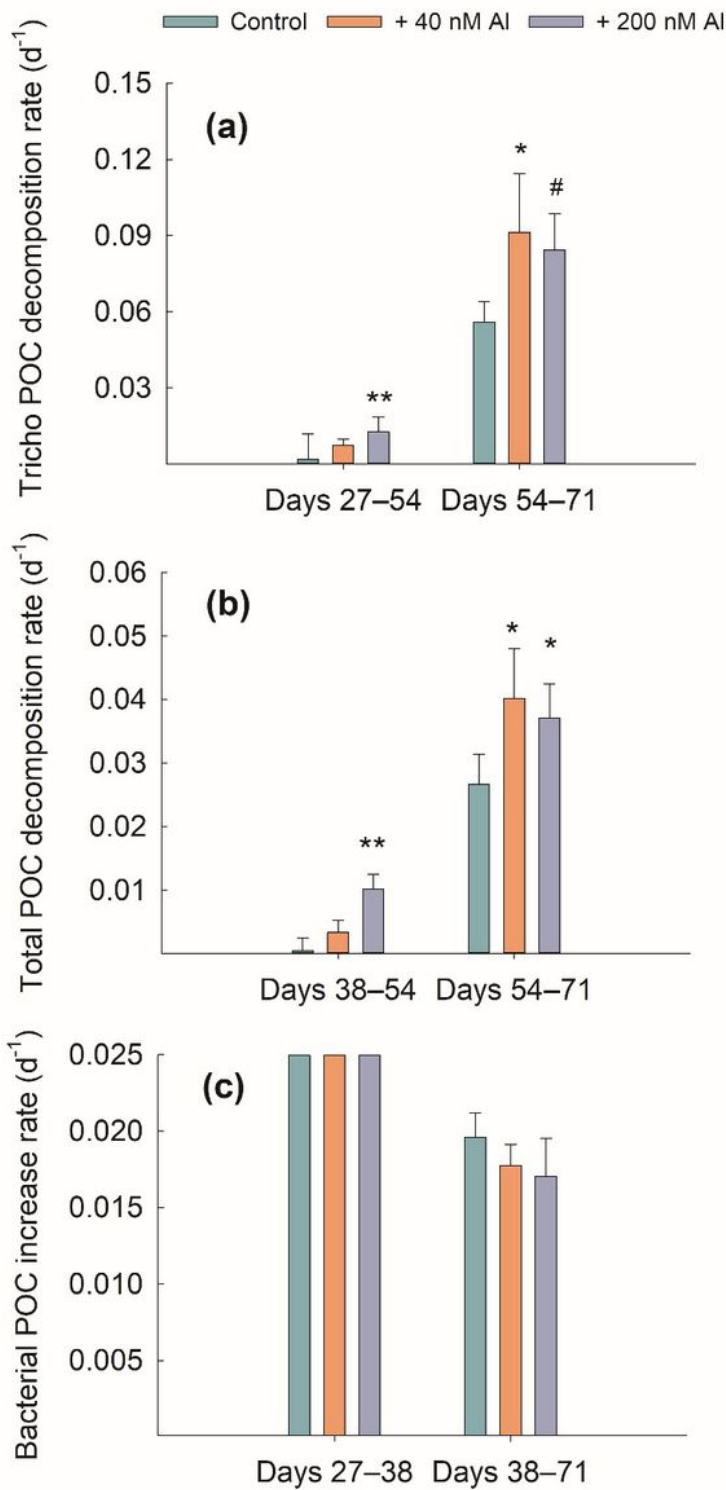


Figure 3

Decomposition rates for particulate organic carbon (POC) in the first decay phase from day 27 to day 71: (a) Tricho POC; (b) total POC; (c) bacterial POC. The error bars represent the standard deviations (n = 3). The symbols #, *, and ** indicate nearly significant ($0.05 < p < 0.1$), significant ($p < 0.05$), and extremely significant ($p < 0.01$) differences compared to the control, respectively. *Trichodesmium* POC and total POC began to decrease on days 27 and 38, respectively. Both exhibited relatively lower decomposition

rates until day 54, after which they decomposed at relatively higher rates until day 71. The bacterial POC increased at high rates during days 27–38.

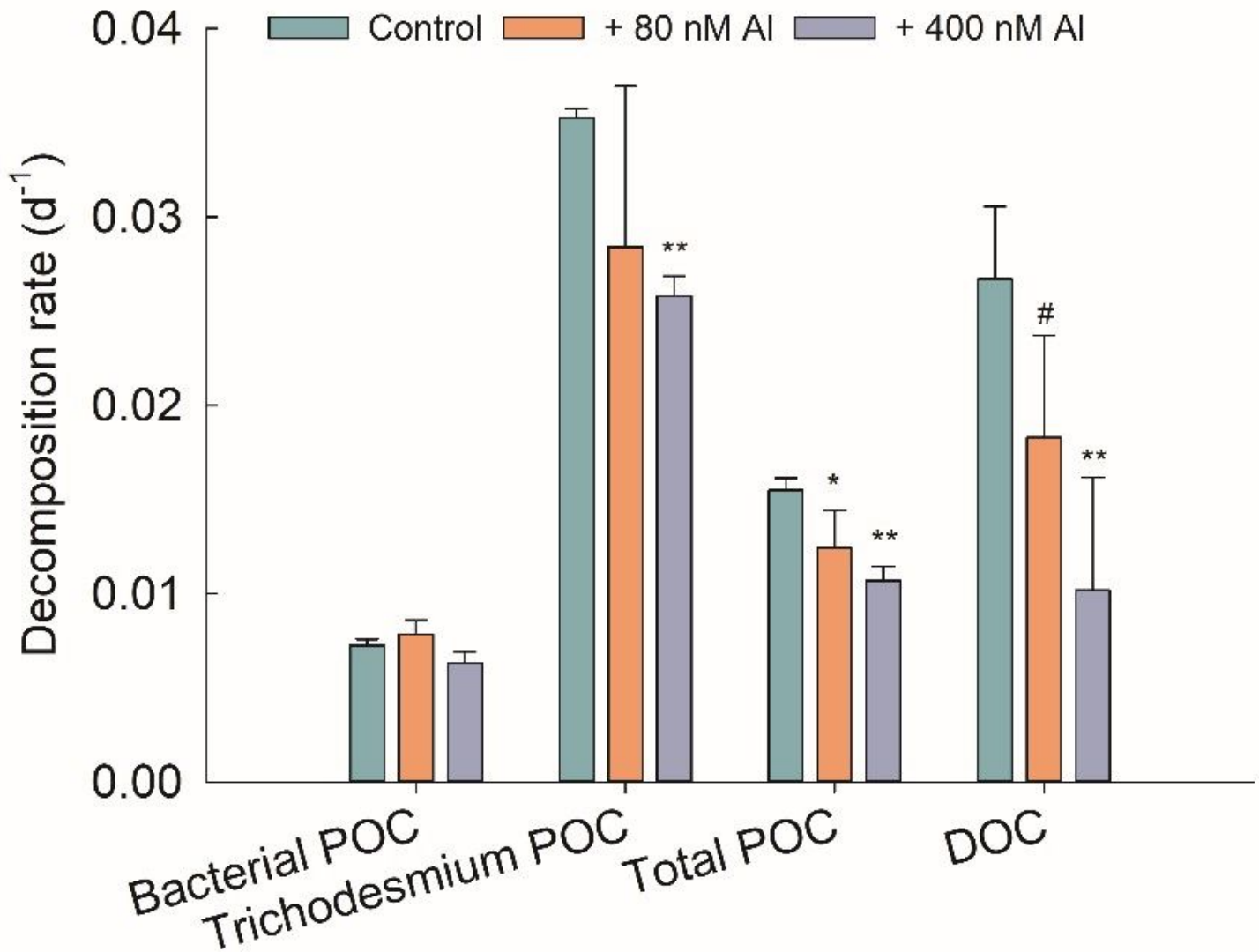


Figure 4

Decomposition rates of organic carbon during the second decay phase from day 71 to day 116, i.e., after the re-addition of Al. The error bars represent the standard deviations (n = 3). The symbols #, *, and ** indicate nearly significant (0.05 < p < 0.1), significant (p < 0.05), and highly significant (p < 0.01) differences compared to the control, respectively.

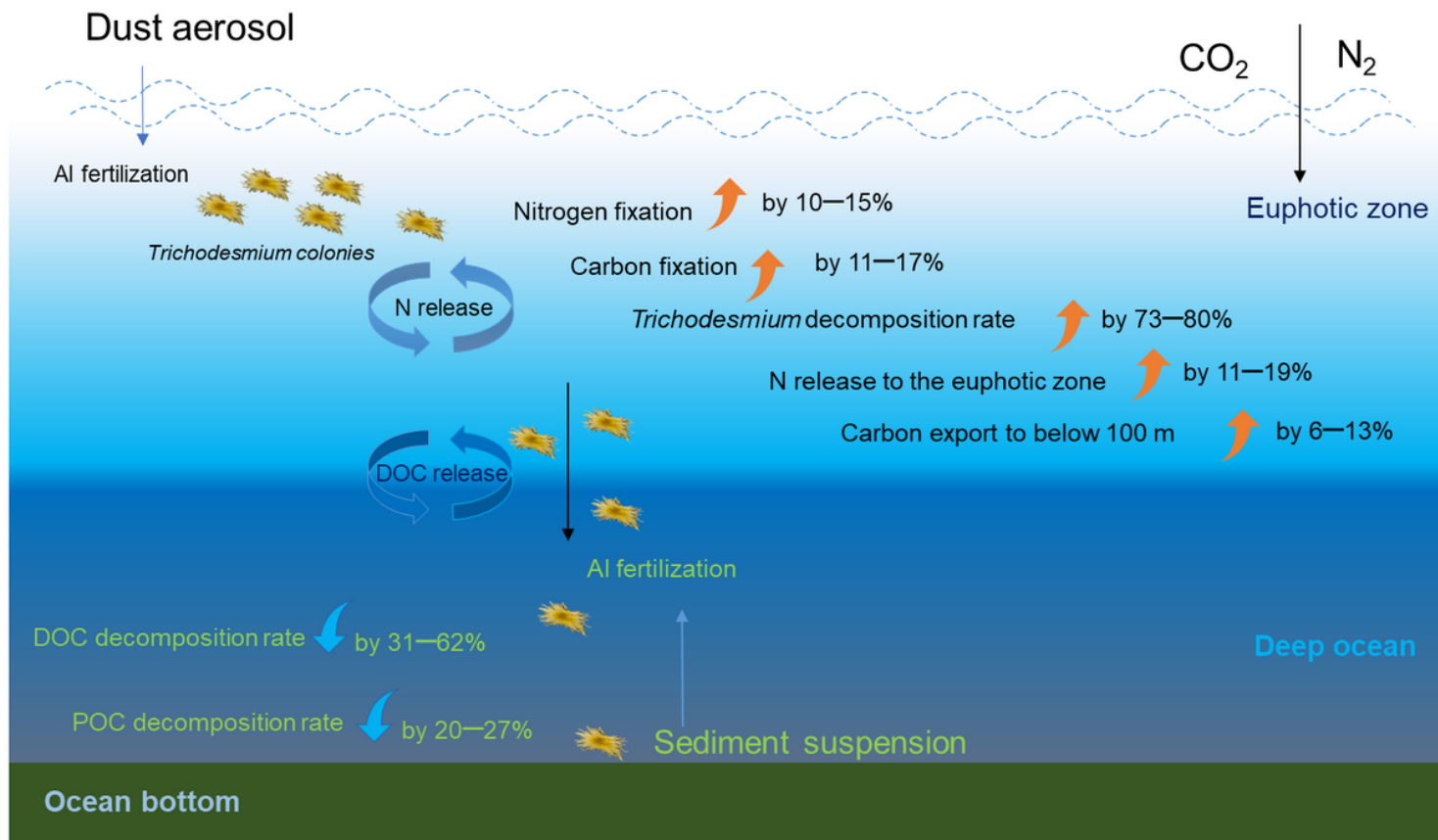


Figure 5

Schematic map showing the estimated effects of Al fertilization from dust deposition and sediment resuspension on the carbon fixation, nitrogen release, carbon export, and decomposition of *Trichodesmium*. The estimates were based on the present experimental data and reported knowledge in the literature (see details in the text).

Supplementary Files

This is a list of supplementary files associated with this preprint. Click to download.

- [SupplementaryInformation20230405.docx](#)